Numerical analysis of CO₂-water separation in a horizontal double T-junction

Milad Amiri [1*], Pawel Ziolkowski[1*], Kamil Stasiak[1] , Dariusz Mikielewicz[1]

[1] Faculty of Mechanical Engineering and Ship Technology, Institute of Energy, Gdańsk University of Technology, 80-233 Gdańsk, Poland

e-mail: milad.amiri@pg.edu.pl, pawel.ziolkowski1@pg.edu.pl, kamil.stasiak@pg.edu.pl, dariusz.mikielewicz@pg.edu.pl

Abstract

Carbon dioxide is considered one of the main factors leading to global warming. Considering the significant impacts of CO_2 on climate change, various technologies have been developed in recent decades to control carbon emission, such as for example CO_2 capture and storage. The developed cycle of a negative CO_2 emission power plant includes some devices, out of which, separator plays an indispensable role. To this end, T-junction separator is widely used as a phase separation component to separate two-phase flow because of its simple structure and low cost. Previous studies suggest that an increase in the number of T-junction branches is conducive to raise phase separation efficiency. In this paper, the numerical simulation in a single T-junction separator is compared with the predicted values generated by experimental models based on air-water. Then, air has been replaced with CO_2 and such separation process in a double T-junction separator has been scrutinized. In addition, the pressure distribution and phase separation performance of two-phase flow of CO_2-water in a horizontal double T-junctions is studied.

1 Introduction

As a phase separator and component separator, T-junction is widely used in petroleum [1], refrigeration systems [2], nuclear reactors [3] and other engineering applications because of its simple structure, small volume and low cost. Śliwicki and Mikielewicz [4] analyzed gas-liquid two-phase flow in a T-junction with a horizontal side tube assuming an annular mist flow pattern at the inlet to the T-junction. Xu et al.[5] proposed a novel construction method of thermodynamic cycle using the T-junction as component separators, which can improve the cycle efficiency of available energy by 22% [6] compared with the

traditional thermodynamic cycle. There are many factors that affect the phase separation of T-junction. Yang et al. [7] summarized these influencing factors as direct factors and basic factors. Direct factors include geometric factors and working conditions, whereas the basic factors are surface tension, inertia force, centrifugal force and gravity. The basic factors are the dominant factors that affect the phase separation and are affected by direct factors. Noor et al. [8] studied the phase separation under five diameter ratios of T-junction with vertical upward branch at different inlet air velocities and liquid velocities through experiments. Results showed that the T-junction with the minimum diameter ratio has the best separation performance under the stratified-wavy flow, but the diameter ratio corresponding to the optimal separation performance is different for different inlet flow pattern.

The phase separation efficiency of a single T-junction, especially the horizontal branching T-junction, is limited. Some literature [7, 9] suggests that the high phase separation efficiency can be achieved by increasing the number of branches. Mohamed et al. [10] carried out a series of experimental studies on the complete phase separation with air-water of a single impacting T-junction at different outlet inclinations, and the results indicated that complete phase separation could not be achieved for a single T-junction at high inlet flow rate, and it might be achieved by introducing multiple T-junctions. Noor and Soliman [8] split the air-water annular flow into two vertical impacting T-junctions and the inlet velocity of two phases was studied when full phase separation could be achieved. When the inlet air velocity is fixed, the liquid phase velocity range of two T-junctions for complete phase separation is almost twice that of a single T-junction. The influence of diameter ratio, separation distance of two branches and inlet velocity on phase separation in branching T-junction with horizontal inlet and vertically upward-downward branches was studied by Wren and Azzopardi [11]. The results showed that when the inlet velocity is low, the separation distance of double regular T-junctions will affect the phase separation, and when the distance decreases, the gas-phase fraction in the downward branch will increase. The phase distribution in horizontal multi-parallel micro-channels was studied by Liu et al. [12]. The effects of five combinations of the orientations of the header and branches on the two-phase flow distribution were compared, and Liu et al. [13] found that the direction of the branches has a great influence on the phase distribution. For annular flow, when the branches are vertically downward, the multiple T-junctions have the highest phase separation efficiency. At present, most of the researches on multiple T-junctions are micro-scale, which is the channel with diameter less than 0.82 mm [14]. However, the factors affecting the phase separation in micro-scale and macro-scale are quite different [7], so it is necessary to increase research investment in macro-scale multiple T-junctions.

Many scholars have studied the phase separation in T-junction, but most of these studies use air-water or steam-water, only a few studies focus on the separation of CO_2-water which could be useful for implementation in the considered by authors negative CO_2 emission gas power plant [15-16]

In this paper separation performance of horizontal T-junction separator has been investigated. Firstly, effect of inlet quality and mass flow rate on distribution of pressure distribution is investigated. Then, the impact of parameters including different inlet mass flow rate and inlet quality on phase of two branches is considered. Finally, separation performance comparison between a single T-junction and double T-junction is presented.

2 Modeling

The 3D single and double T-junction geometry are shown in Figs. 1 and 2, respectively. The length of each leg is 0.5 m. In addition, the distance between two branches is 1 m in double T-junction separator. The diameter is 3.81 cm. The parameters are consistent with the parameters set out in Saba et al. [17]. CO_2-water are the working fluids. Boundary conditions include velocity inlet and outflow outlet. The exit boundary conditions of the outlet and branch pipe are expressed as follows:

$$\frac{du}{ds} = 0$$
$$\frac{dp}{ds} = constant$$

(1)

where u is velocity along the flow direction, s is parallel to the direction of u and p is a static pressure. The outflow boundary conditions for the exits of outlet and branch pipe imply a zero diffusion flux for all flow variables and an overall mass balance correction. The zero diffusion flux condition applied at outflow cells means that the conditions of the outflow plane are extrapolated from within the domain and have no impact on the upstream flow. The extrapolation procedure updates the outflow velocity and pressure in a manner that is consistent with a fully-developed flow assumption. All solid boundary walls are smooth and adiabatic and are assumed to possess a no-slip boundary condition. The gravity acceleration 9.81 m·s^{-2} is considered in the converse direction of y.

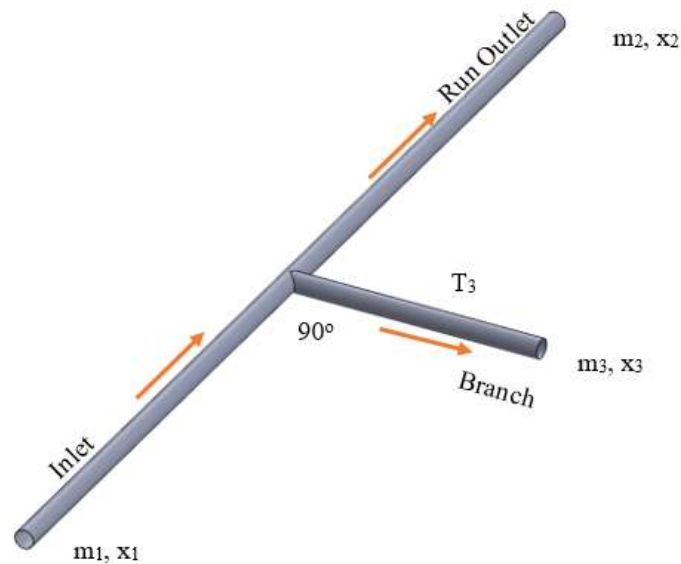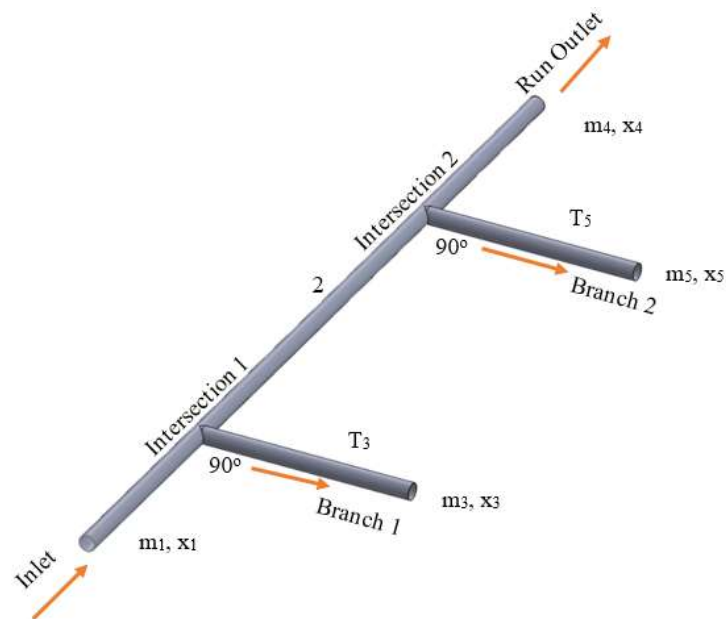*Figure 1: Single T-junction geometry, m: mass flow rate (g/s) and x: inlet flow quality*

Figure 2: Double T-junction geometry, m: mass flow rate (g/s) and x: inlet flow quality

2.1 Governing equations and boundary conditions

An Eulerian-Eulerian model is used, which considers the two phases as continuum and phase coupling. There is no mass transfer and heat exchange between the two phases. The wall is smooth and adiabatic. The non-equilibrium equation is used to calculate the near wall flow.

The continuity equations are expressed by:

$$\nabla.\left(\alpha_{ph}\rho_{ph}\mathbf{V}_{ph}\right) = 0 \tag{2}$$

The gas is set as the primary phase, the liquid is the secondary phase, and the relationship between two phases can be written by:

$$\sum \alpha_{ph} = 1 \tag{3}$$

α_{ph} is the void fraction, and ph denote gas or liquid. Momentum conservation equations are written as:

$$\nabla.\left(\alpha_{ph}\rho_{ph}\mathbf{V}_{ph}\mathbf{V}_{ph}\right) = -\alpha_{ph}\nabla p + \nabla.\tau_{ph} + \alpha_{ph}\rho_{ph}\mathbf{g} + \mathbf{f} + \mathbf{S}$$

$$\tau_{ph} = \alpha_{ph}\left(\mu_{ph} + \mu_{t,m}\right)\left(\nabla\mathbf{V}_{ph} + \nabla\mathbf{V}_{ph}^T\right) + \alpha_{ph}\left(\lambda_{ph} - \frac{2}{3}\left(\mu_{ph} + \mu_{t,m}\right)\right)\nabla.\mathbf{V}_{ph}\mathbf{I} \tag{4}$$

P is the static pressure, g is the gravitational acceleration, S is the surface tension, f is the drag force coefficient which can be calculated by:

$$f = \frac{C_D Re}{24}$$

$$C_D = \begin{cases} 24(1 + 0.15Re^{0.678})/Re & Re \leq 1000 \\ 0.44 & Re \geq 1000 \end{cases} \tag{5}$$

$$Re = \rho_G |v_L - v_G| d_p/\mu_G$$

The droplet diameter d_p is 10^{-5}. Boundary conditions include velocity inlet and outflow outlet. The inlet velocity can be calculated by:

$$v_G = m_1 x_1/\rho_G \alpha_G$$

$$v_L = m_1(1 - x_1)/\rho_L \alpha_L \tag{6}$$

The standard k-ε turbulence model is used to simulate the flow.

$$\nabla.(\rho_m\mathbf{V}_m k) = \nabla.\left(\left(\mu_m + \frac{\mu_{t,m}}{\sigma_k}\right)\nabla k\right) + G_{k,m} - \rho_m\varepsilon$$

$$\nabla.(\rho_m\mathbf{V}_m\varepsilon) = \nabla.\left(\left(\mu_m + \frac{\mu_{t,m}}{\sigma_\varepsilon}\right)\nabla\varepsilon\right) + \frac{\varepsilon}{k}\left(C_1 G_{k,m} - C_2\rho_m\varepsilon\right) - R_\varepsilon \tag{7}$$

$\sigma_k, \sigma_\varepsilon, C_1$ and C_2 are 1, 1.3, 1.44 and 1.92, respectively. ρ_m is the density of the mixture, $\mu_{t,m}$ is the turbulent viscosity of the mixture and $\mathbf{V}_m$ is the mixture velocity. They are defined as:

$$\rho_m = \sum_{ph=1}^{N} \alpha_{ph}\rho_{ph}$$

$$\mu_m = \sum_{ph=1}^{N} \alpha_{ph}\mu_{ph}$$

$$\mathbf{V}_m = \sum_{ph=1}^{N} \alpha_{ph}\rho_{ph}\mathbf{V}_{ph} / \sum_{ph=1}^{N} \alpha_{ph}\rho_{ph} \tag{8}$$

$$\mu_{t,m} = \rho_m C_\mu k^2/\varepsilon$$

In eq. (8) $C_\mu = 0.0845$ and N includes 1 (gas) and 2 (liquid). $G_{k,m}$ represents turbulent kinetic energy due to average gradient, and can be expressed by:

$$G_{k,m} = \mu_{t,m}[\nabla\mathbf{V}_m + \nabla\mathbf{V}_m^T]/\nabla\mathbf{V}_m \tag{9}$$

A steady pressure-based solver is used to solve the conservation equations. First order upwind method is applied to spatially disperse the momentum, turbulent kinetic energy, turbulent dissipation rate and volume fraction. The criterion of convergence is that the residual is reduced to $10-5$ and the mass flow rate at each outlet is stable.

3 Numerical calculations

3.1 Grid independence

Grid-independence leads to calculational results change along with a denser or looser grid that the truncation error can be ignored in numerical simulation. It should be noted that the grid independence should be investigated in areas where the purpose of the simulation is to study them or they have a significant effect on the results. The geometry of single and double T-junction separator has been simulated in GAMBIT in 3D. Figure 3 and 4 shows the geometry and its mesh. To ensure that the solution is independent of the mesh resolution, a mesh sensitivity analysis is carried out for single T-junction separator. Four meshes shown in Table 1 are investigated. It can be observed that the pressure drop does not change for mesh 3 and mesh 4. Therefore, Mesh3 is chosen as the calculation mesh.

Table 1: Mesh independency

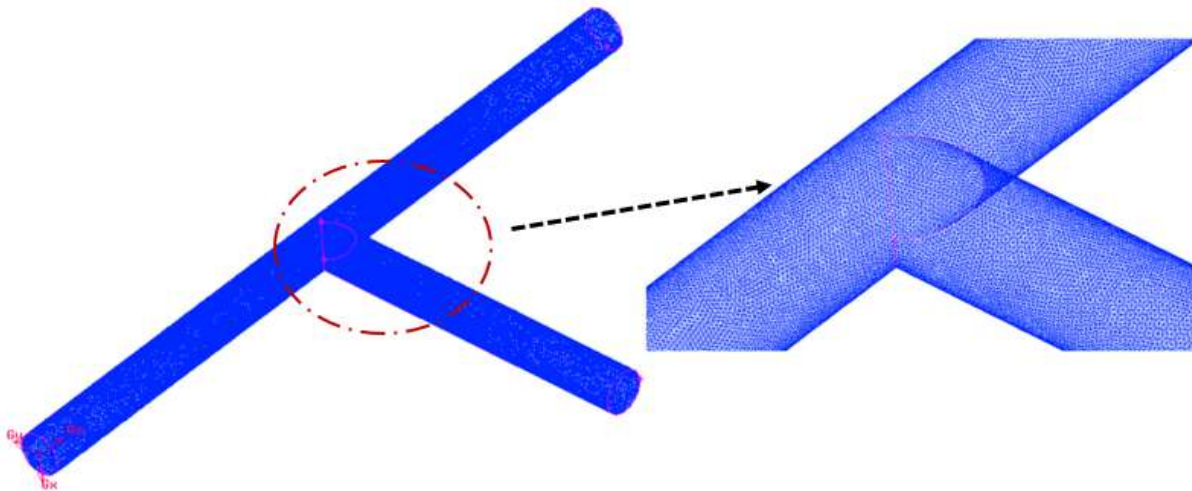| Grids	Mesh1	Mesh2	Mesh3	Mesh4
Nodes	500,000	750,000	1,000,000	1,250,000
$(\Delta p_{2-1})_j$	3300	3450	3510	3510

Figure 3: Simulation of single T-junction in GAMBIT

3.2 Model validation

In this part, T-junction separator has been simulated and the obtained results were validated with experimental work (Saba et all, 1984). The experimental paper claimed that the analysis of light water nuclear reactor (LWR) loss-of-coolant accidents (LOCAs) requires that one be able to accurately calculate the two-phase flow splits in complex, branching conduits. The tee test section was designed and constructed from Plexiglas, to allow for observation of the phenomena. It was installed (horizontally) in a large air/water loop at Rensselaer Polytechnic Institute (RPI). The data consisted of the various air and water inlet and outlet flows, the pressure gradients and the inlet pressure. Using the measured pressure gradients, the differential pressure at the tee junction was obtained by extrapolation. In all cases, side 1 is the entrance, side 2 is the run, and side 3 refers to the branch. There are 45 different runs in experimental work. Two of them simulated by FLUENT to validate our numerical modelling

with experimental conditions. For this purpose, run 1 and 10 (Table2) have been chosen. It can be seen that flow regime in Run1 is single phase, so it means that liquid phase (water) is simulated.

Table 2: Phase separation data in a horizontal Tee (Experimental Work-Saba et all, 1984)

Run	$G_1 \times 10^6$	$x_1(\%)$	$x_2(\%)$	$x_3(\%)$	$\dfrac{w_2}{w_1}$	$p_1(kPa)$	$(\Delta p_{2-1})_j$ (kPa)
1	4.88	0	0	0	0.3	41.37	0.89
10	4.88	0.5	0.0130	0.695	0.3	48.26	3.51

Diagram of static pressure along inlet and run section for runs 1 and 10 is indicated in Fig 4, respectively. It can be seen that in accordance with table 1, ΔP_{2-1_j} is 890 and 3510 Pascal respectively and Fig. 4 show very acceptable results.
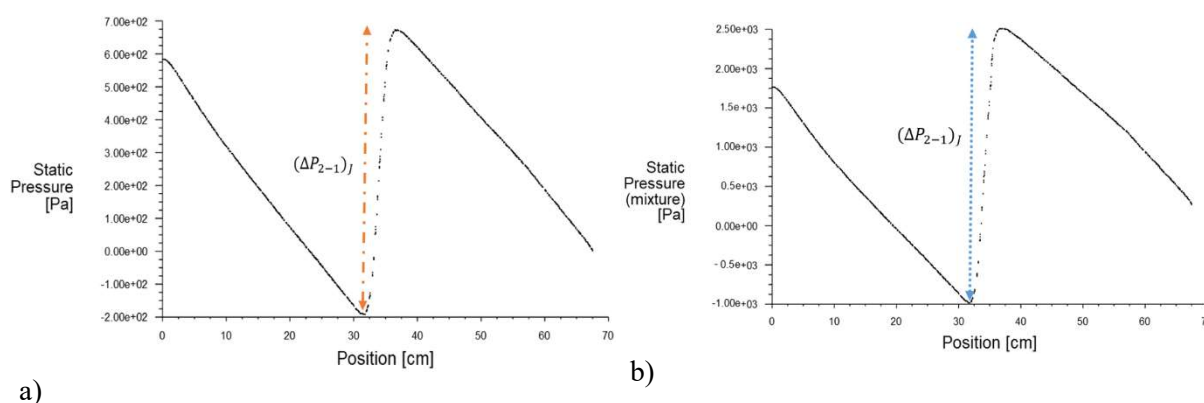

a)

b)

Figure 4: Distribution of static pressure of a) Run1 and b) Run10 in numerical simulation

4 Results and discussion

4.1 Effect of inlet quality and mass flow rate

Figure 5 presents distribution of pressure for different inlet quality when m1 is equal to 15 (g/s) of CO2 and water. It can be seen that rising inlet flow quality leads to increasing the local pressure drop in both branches, so that the first branch has been faced with faster decreasing of pressure in comparison to the second one. Figure 6 shows the effect of inlet mass flow rate on distribution of pressure when inlet flow quality is 0.3. It can be considered that the trend the inlet mass flow rate also exhibits the same trend as the inlet quality. Increasing of inlet mass flow rate and quality results in rising the velocity of two phases, which, in turn, is prone to generate more kinetic energy loss due to violent collision. So, the greater the inlet mass flow rate causes the larger the local pressure drop at the intersection.
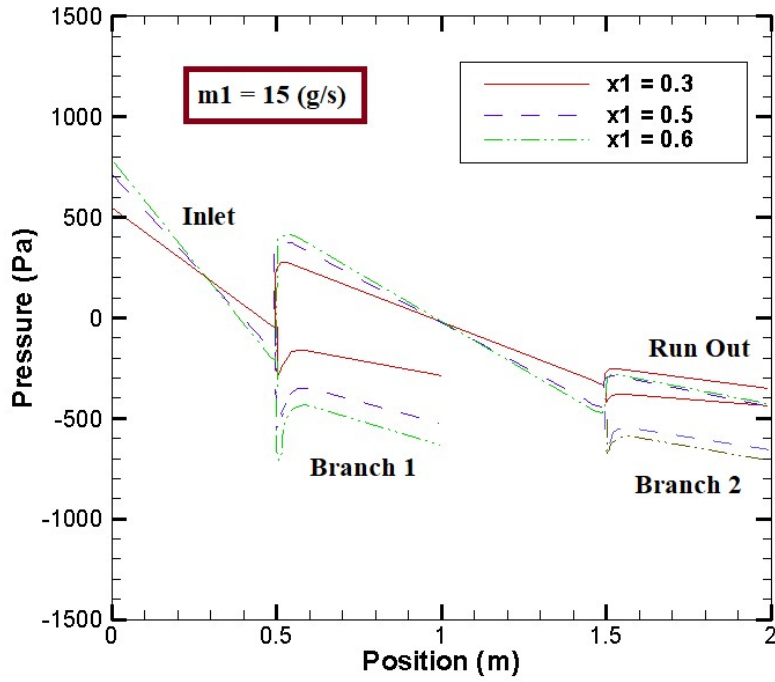
Figure 5: Distribution of pressure for different inlet quality at m1=15 g/s
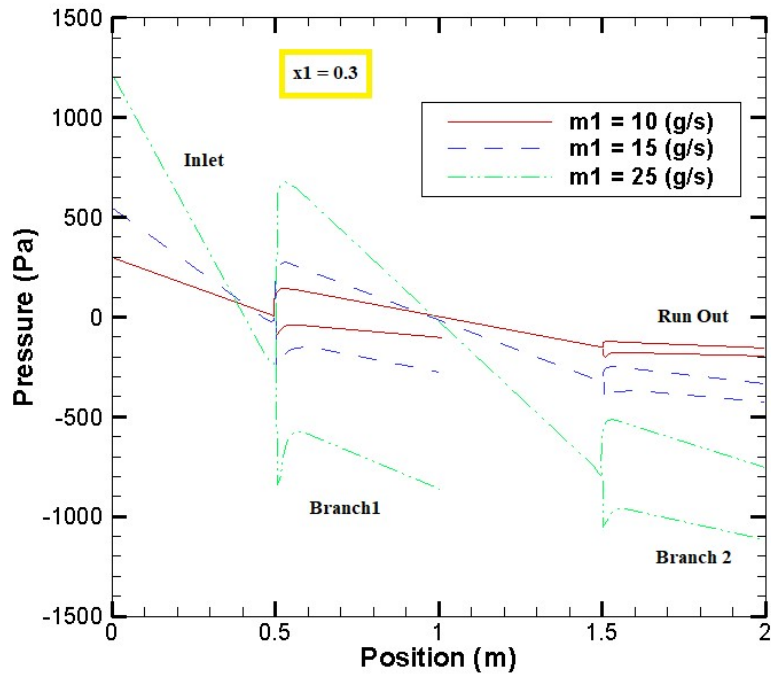

Figure 6: Distribution of pressure for different inlet mass flow rate at x1=0.3

4.2 Effects of parameters on phase of two branches

To evaluate the phase separation performance of each outlet, the mass flow rate ratio of gas (F_G), the mass flow rate ratio of liquid (F_L) and the total mass flow rate ratio including gas and liquid (Fi) are defined by:

$$F_G = \frac{F_{Gi}}{F_{G1}}, \ F_L = \frac{F_{Li}}{F_{L1}}, F_i = \frac{F_i}{F_1} \tag{10}$$

Figure 7 indicates the effect of inlet quality on phase separation performance for both branches at m1=15 (g/s). As it is shown, although with increasing inlet flow quality the phase separation of the first branch

is less affected, the increase of inlet quality enhances the gas phase separation of first branch. On the other hand, increase of x1 leads to decreasing of the gas phase separation parameters of second branch.
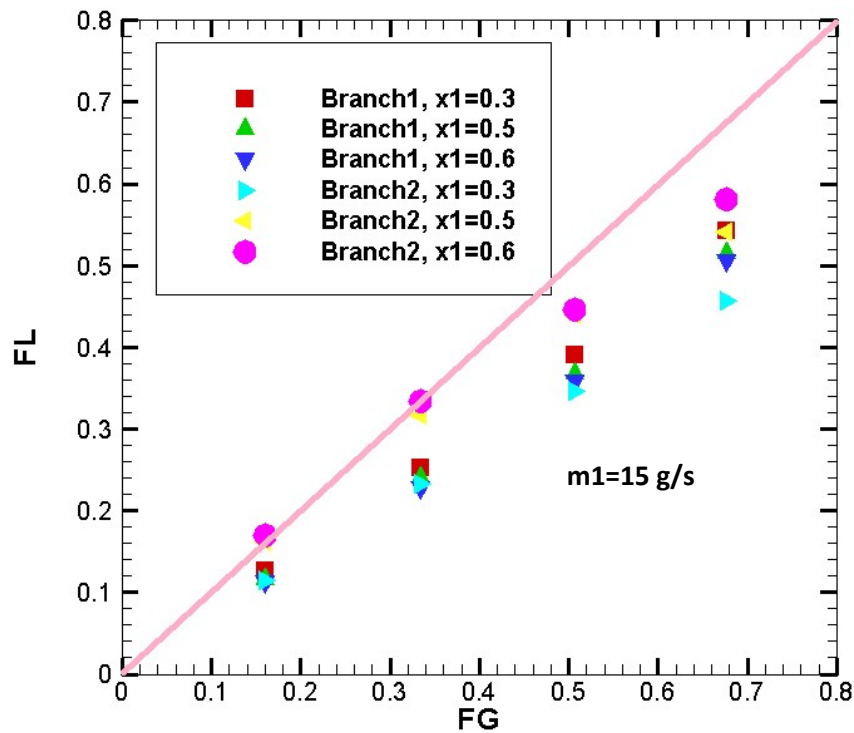

Figure 7: Phase separation performance for different inlet quality

Figure 8 shows the effect of inlet mass flow rate on phase separation performance at x1=0.3. It can be observed the change of inlet mass flow rate has little influence on the phase separation parameters of the first branch, whilst the gas-phase separation of the second branch rises obviously with the decrease of m1.
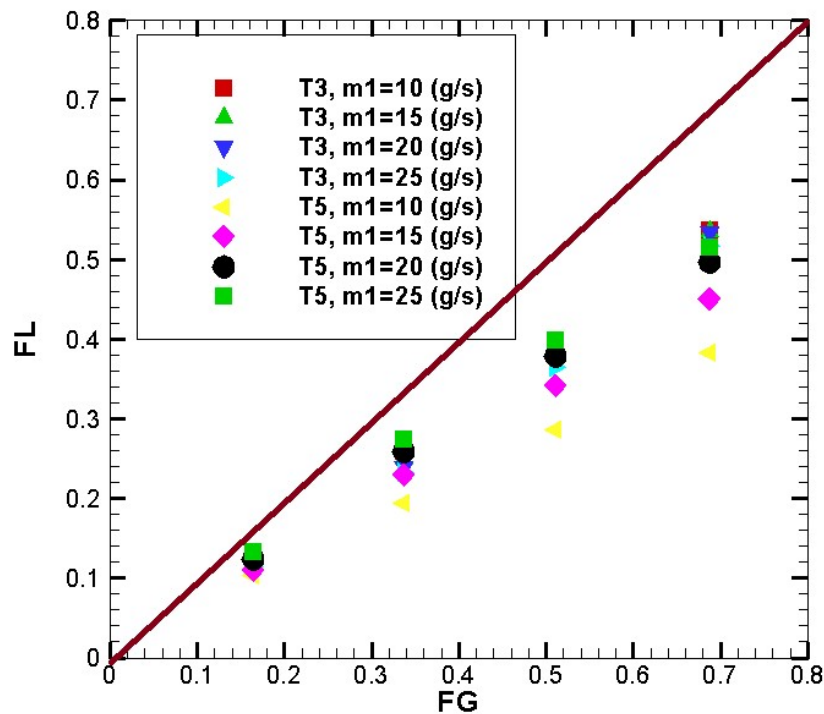

Figure 8: Phase separation performance for different inlet mass flow rate at x1=0.3

4.3 Comparison of separation performance between single T-junction and double T-junction

In order to present the performance of phase separation more directly, the concept of phase separation efficiency has been introduced, which is the absolute value of the difference between F_G and F_L, as expressed as follows:

$$\eta = |F_G - F_L| \tag{11}$$

T_3 and T_5 branches are considered as a whole part T_{35} in the study of separation performance of double T-junction and single T-junction. In this part, m_4 is set at a constant value, i.e. the sum of m_3 and m_5 is fixed. The numerical results are depicted in Fig. 9. It can be seen that double T-junction can effectively boosts the phase separation efficiency in the low mass split ratio $\left(\frac{m_{35}}{m_1}\right)$, while double T-junction has no promoting impact in high mass split ratio. In some cases, at high mass split ratio, only single T-junction can achieve the highest separation performance limit and there is no need to use another branch to promote the separation performance, so the separation efficiency of double T-junction is even worse than that of single T-junction.
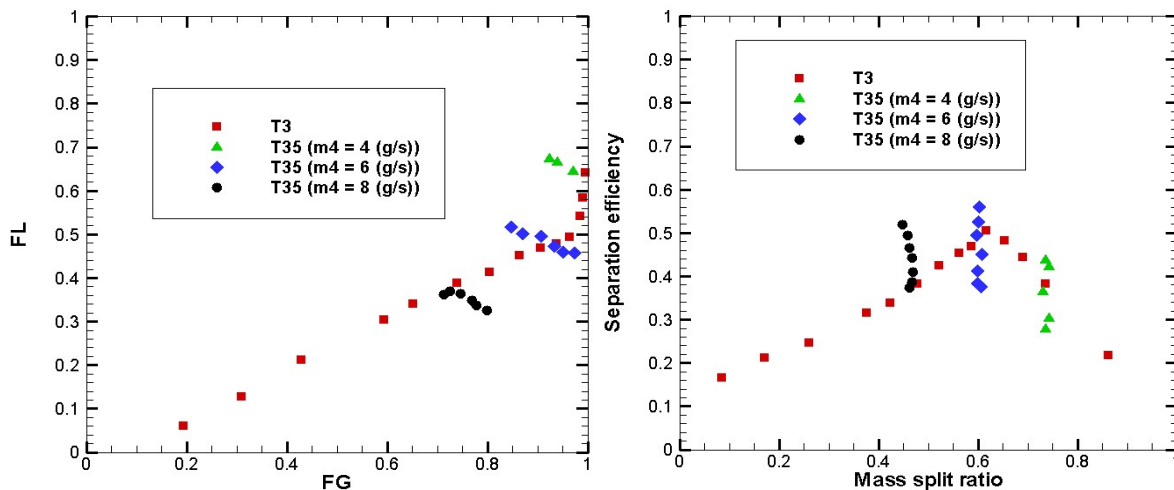
Figure 9: Comparison of phase separation performance between double T-junction and single T-junction at x_1=0.3 and m_1=15 (g/s)

5 Conclusion

In this paper, the pressure distribution of the two-phase flow of CO_2-water in the double T-junctions are studied. Furthermore, effects of inlet quality and mass flow rate on both branches as well as comparison of separation performance of single and double T-junction separator investigated. The conclusions are shown as follows.

- Increasing of x_1 and m_1 leads to rise the local pressure at the intersections.
- The phase separation of the first branch is less affected with increasing inlet flow quality.
- Increase of inlet flow quality results in decreasing of the gas phase separation parameters of second branch.
- The gas-phase separation of the second branch rises obviously with the decrease of m1.
- Double T-junction can effectively boost the phase separation efficiency in the low mass split ratio, while double T-junction has no promoting impact in high mass split ratio

Acknowledgements

References

[1]   Abbad, M., et al. *In-line water separation: a new promising concept for water debottlenecking close to the wellhead*. in *SPE Middle East Oil & Gas Show and Conference*. 2015. OnePetro.

[2]   Tuo, H. and P. Hrnjak, *Vapor–liquid separation in a vertical impact T-junction for vapor compression systems with flash gas bypass*. International journal of refrigeration, 2014. 40: p. 189-200.

[3]   Welter, K., et al., *Experimental investigation and theoretical modeling of liquid entrainment in a horizontal tee with a vertical-up branch*. International journal of multiphase flow, 2004. 30(12): p. 1451-1484.

[4]   Sliwicki, E. and J. Mikielewicz, *Analysis of an annular-mist flow model in a T-junction*. International journal of multiphase flow, 1988. 14(3): p. 321-331.

[5]   Xu, W., et al., *How to approach Carnot cycle via zeotropic working fluid: Research methodology and case study*. Energy, 2018. 144: p. 576-586.

[6]   Xu, W., et al., *Performance analysis on novel thermodynamic cycle under the guidance of 3D construction method*. Applied Energy, 2019. 250: p. 478-492.

[7]   Yang, B., et al., *State-of-art of branching T-junction: Experiments, modeling, developing prospects and applications*. Experimental Thermal and Fluid Science, 2019. 109: p. 109895.

[8]   Noor, S. and H.M. Soliman, *Experimental investigation of phase-separation effectiveness of combined impacting tee junctions*. International Journal of Mechanical Engineering and Robotics Research, 2019. 8(3).

[9]   Yang, L., et al., *Phase separation of gas–liquid two-phase stratified and plug flows in multitube T-junction separators*. AIChE Journal, 2017. 63(6): p. 2285-2292.

[10]   Mohamed, M., H. Soliman, and G. Sims, *Conditions for complete phase separation in an impacting tee junction at various inclinations of the outlet arms*. International Journal of Multiphase Flow, 2012. 47: p. 66-72.

[11]   Wren, E. and B. Azzopardi, *The phase separation capabilities of two T-junctions placed in series*. Chemical Engineering Research and Design, 2004. 82(3): p. 364-371.

[12]   Liu, Y., W. Sun, and S. Wang, *Experimental investigation of two-phase slug flow distribution in horizontal multi-parallel micro-channels*. Chemical Engineering Science, 2017. 158: p. 267-276.

[13]   Liu, Y., et al., *Gas-liquid two-phase flow distribution in parallel micro-channels with different header and channels' orientations*. International Journal of Heat and Mass Transfer, 2017. 112: p. 767-778.

[14]   Chen, J.-l., et al., *Simulation of oil-water two phase flow and separation behaviors in combined T junctions*. Journal of Hydrodynamics, 2012. 24(6): p. 848-857.

[15]   Ziółkowski, P., et al., *Thermodynamic Analysis of Negative CO2 Emission Power Plant Using Aspen Plus, Aspen Hysys, and Ebsilon Software*. Energies, 2021. 14(19): p. 6304.

[16]   Wrzesień, S., P. Madejski, and P. Ziółkowski, *Computational Fluid Dynamics Simulation of Gas–Liquid Multiphase Flow in T-junction for CO2 Separation*. Prace Naukowe Wydziału Architektury Politechniki Wrocławskiej, 2021: p. 403-414.

[17]   Saba, N. and R.T. Lahey Jr, *The analysis of phase separation phenomena in branching conduits*. International journal of multiphase flow, 1983. 10(1): p. 1-20.